Astron. Astrophys. 322, 591–597 (1997)

ASTRONOMY
AND
ASTROPHYSICS

Hot high-gravity NLTE model atmospheres as soft X-ray sources

H.W. Hartmann and J. Heise

SRON Laboratory for Space Research, Sorbonnelaan 2, 3584 CA Utrecht, The Netherlands

Received 31 October 1996 / Accepted 3 December 1996

Abstract. Hot optically thick plasmas in the temperature range $10^5 < T_{\rm eff} < 10^6$ K emit soft X-rays ($\sim 0.1 - 1$ keV). The spectra are in zero order often approximated with blackbodies. Considering LTE-atmospheres as a better first order approximation Heise et al. (1994) show that these atmospheres are more efficient X-ray emitters than blackbodies.

In this paper we study the assumption of Local Thermodynamic Equilibrium (LTE) and present calculations of unblanketed, hot, high-gravity Non-LTE (NLTE) model atmospheres in hydrostatic and radiative equilibrium. The range of temperatures is chosen such that they emit significantly in the soft X-ray range ($0.1 - 2.0$ keV). The gravitational fields of $g = 10^{7.5} - 10^{10}$ cm s^{-2} are applicable to massive white dwarfs. It appears that NLTE spectra are comparable to LTE spectra if $\log g \geq 9$, i.e. for the most massive white dwarfs ($M \geq 0.6\,{\rm M}_\odot$). At these gravities the density is sufficiently high to assume that collisional ionizations dominate and that LTE determines the degree of ionizations and the atomic population levels.

We show fits of H, He, C, N, O, Ne NLTE model atmospheres to observed ROSAT spectra of Supersoft Sources (SSS) in the Galaxy and the LMC. The resulting effective temperatures strongly depend on the assumed model parameters, such as the gravity and the metallicities. With the present X-ray spectral resolution, temperature, gravity and abundances cannot be determined independently.

Key words: stars: atmospheres – accretion – radiative transfer – white dwarfs – X-rays: stars

1. Introduction

Atmospheres of hot white dwarfs are known to emit soft X-rays (0.1 - 2.0 keV). Among the first discoveries are isolated hot DA white dwarfs such as the prototype HZ43, and sources like Sirius B. Supersoft Sources (SSS) belong to another class of X-ray sources that was discovered with the EINSTEIN satellite in the first soft X-ray survey of the Magellanic Clouds (Long et al. 1981). Observations of SSS show extremely soft (0.1 - 2.0 keV) X-ray spectra with typical luminosities between 10^{36} and 10^{38} erg s^{-2}. They exist as persistent and transient sources (e.g. CAL87 and CAL83 respectively) both as isolated stars (e.g. N67) and in binaries. SSSs are divided into relatively 'soft' SSSs with spectra that have the bulk of their flux below 0.5 keV, and relatively 'hard' SSSs that emit mainly above 0.5 keV. Among the latter are CAL87 and RX J0925.7-4758 which will be discussed in Sect. 4.

SSSs are believed to be nuclear burning white dwarfs (van den Heuvel et al. 1992) with characteristic (blackbody) temperatures of $2 \times 10^5 - 1 \times 10^6$ K. Kylafis & Xilouris (1993) and Kylafis (1996) show that neutron stars with extended atmospheres could also explain the observations. SSSs are important candidates for the predecessors of SNe type-Ia.

The spectrum of an optically thick soft X-ray source is often taken as blackbody emission. This is a fair approximation if the opacity as a function of energy is roughly constant. However, in the soft X-ray range the emission spectrum at certain temperatures and densities is often dominated by a few ions, such as the helium and hydrogen-like ions of carbon, nitrogen and oxygen. The atmospheric emission deviates largely from a blackbody at the effective temperature: the atmosphere is transparent for soft X-rays. Optical depth of the order one in the soft X-ray range is reached at a depth where the temperature is much higher than the surface temperature of the atmosphere. In such cases it is necessary to compute plane-parallel model atmospheres in hydrostatic and radiative equilibrium.

Heise et al. (1994) have shown that Local Thermodynamic Equilibrium (LTE) model atmospheres for white dwarfs are more efficient X-ray emitters than blackbodies and consequently that the luminosity of those LTE model atmospheres, if applied to SSSs, could stay below the Eddington limit. They had to assume that at surface gravities of white dwarfs, which are of the order of $10^7 - 10^{10}$ cm s^{-2}, the high density causes the atmosphere to be in thermodynamic equilibrium and that the Saha-Boltzmann law determines the degree of ionization and the atomic level occupation. This assumption may not be valid in the outer low-density region of the atmosphere where Non-LTE (NLTE) is a better assumption.

Dreizler & Werner (1993) were the first to calculate fully self-consistent metal line-blanketed NLTE model atmospheres

Send offprint requests to: w.hartmann@sron.ruu.nl

for white dwarfs up to $T_{\rm eff} = 10^5$ K and $6 \leq \log g \leq 7.5$. They used the obtained spectra to interpret EUV observations. Jordan et al. (1994, 1996) fitted line blanketed, state-of-the-art NLTE models in the range $T_{\rm eff} < 4 \times 10^5$ K and $5 \leq \log g \leq 7$ to the SSSs RR Tel and SMC3.

We present NLTE models with effective temperatures in the range $3 \times 10^5 - 1 \times 10^6$ K. The main purpose of this paper is to compare the differences between blackbody, LTE and NLTE spectra, to explore how the soft X-ray emission of NLTE model atmospheres changes as a function of gravity, effective temperature and abundance. We will apply our models to several ROSAT spectra of SSSs.

2. Model atmospheres

We calculate NLTE models in radiative and hydrostatic equilibrium with cosmic (Allen 1973), LMC and SMC (Dennefeld 1989) abundances for He, C, N, O and Ne. We will include heavier elements in future models.

The gravity ranges from $\log g = 7.5$ to $\log g = 10$ in steps of 0.5. The effective temperature is limited by the surface gravity via the Eddington limit, since the model atmosphere would no longer be hydrostatic at higher effective temperatures. We calculate effective temperatures from 3×10^5 K up to 4×10^5 K for $\log g = 7.5$ and up to 1.08×10^6 K for $\log g = 9$ in steps of 1×10^4 K.

The model atmospheres are calculated using the computer code TLUSTY178 (Hubený 1988, Hubený & Lanz 1995). This code uses the complete linearization technique to solve the coupled set of radiative transfer, radiative equilibrium and statistical equilibrium equations. The difference equation of the radiative transfer equation is represented by the standard Feautrier scheme. Convergence is achieved when the relative changes of the temperature, total number density and electron density are smaller than 5×10^{-3}. For a detailed description of the computer code TLUSTY178 we refer to Hubený (1988) and Hubený & Lanz (1995).

The models are calculated on 70 depth points and a frequency grid containing 268 points including frequencies just above and below threshold ionization energies. The frequency range runs from 10^{15} (~ 4 eV) to 2×10^{18} (~ 8.3 keV) Hz.

Lanz & Hubený (1995) show for carbon and iron that metal line opacities have to be taken along in NLTE model atmosphere calculations. They conclude that line blanketing by trace elements with abundances above 10^{-5} times solar influences the atmospheric structure of hot, metal-rich white dwarfs. Rauch (1996) calculated line-blanketed NLTE model atmospheres up to $T_{\rm eff} = 4 \times 10^5$ K, to show that light metal opacities drastically decrease the flux levels of hot stars.

For now, we ignore line opacities and line blanketing. We consider those as the next step in the refinement of our models, which should also take expanding atmospheres into account.

Table 1. Model ions in the NLTE calculations. Only the lowest atomic levels, including the ground state, are used

ion	no. of levels	ion	no. of levels
H I	1	O VI	2
H II	1	O VII	3
He II	1	O VIII	3
He III	1	O IX	1
C V	1	Ne VII	3
C VI	3	Ne VIII	2
C VII	1	Ne IX	1
N VI	3	Ne X	1
N VII	3		
N VIII	1		

2.1. Model atoms

We restrict ourselves to a limited number of ionization stages and atomic levels. It appears that the spectrum of hot, high-gravity atmospheres is often dominated by the lowest levels of one or two ionization stages of a particular element. Therefore, we selected those ionization stages that we expected to be most dominant in the range of parameters of interest. See Table 1.

2.2. Treatment of continuum opacities

Photoionization cross-sections of the ground state were determined using data and fitting formula from Verner & Yakovlev (1995):

$$\sigma_{nl}(E) = \sigma_0 F(y) \text{ Mb},$$

$$F(y) = \left[(y-1)^2 + y_{\rm w}^2\right] y^{-Q} \left(1 + \sqrt{y/y_{\rm a}}\right)^{-P}, \quad (1)$$

where n and l are the principal and subshell orbital quantum number respectively, E is the photon energy in eV, $y = E/E_0$. $\sigma_0, E_0, y_{\rm w}, y_{\rm a}$ and P are fit parameters and $Q = 5.5 + l - 0.5P$. The photoionization cross-sections of the excited atomic levels are based on the calculations of Barfield et al. (1972) and Reilman & Manson (1979) using the interpolation formula from Henry (1970). $\nu_{\rm T}$ is the threshold frequency of the transition and σ_0, α and β are fit parameters.

$$\sigma_\nu = \sigma_0 \times 10^{-18} \left[\alpha \left(\frac{\nu}{\nu_{\rm T}}\right)^{-s} + (\beta - 2\alpha) \left(\frac{\nu}{\nu_{\rm T}}\right)^{-s-1} + (1 + \alpha - \beta) \left(\frac{\nu}{\nu_{\rm T}}\right)^{-s-2}\right]. \quad (2)$$

These cross-sections, when calculated for ground states, do not differ by more than 6 % in the energy range of interest ($\sim 0.1 - 2.0$ keV) compared to Verner & Yakovlev.

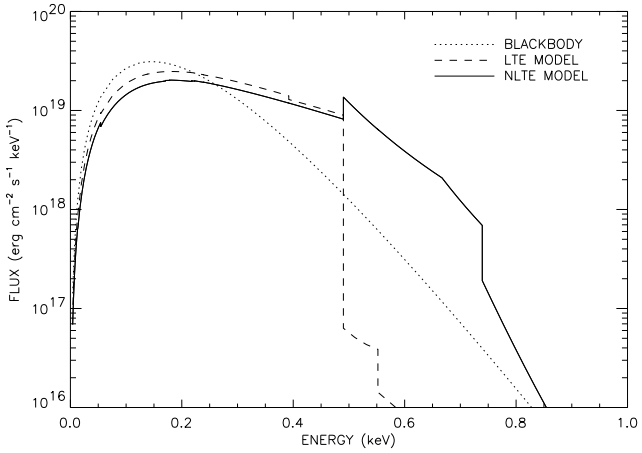

Fig. 1. Blackbody and LTE and NLTE model atmospheres are compared for $\log g = 8.5$ and $T_{\rm eff} = 6 \times 10^5$ K. Abundances are cosmic. Note the transition of the C VI edge (0.49 keV) from absorption to emission when the condition of LTE is relaxed

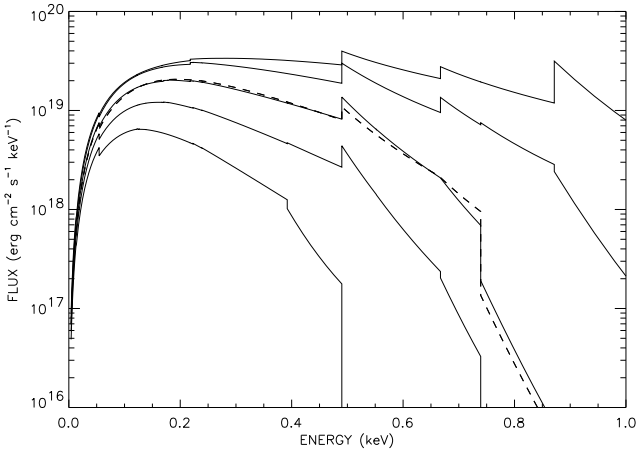

Fig. 2. Solid lines: NLTE model spectra at $\log g = 8.5, 4 \times 10^5 \leq T_{\rm eff} \leq 8 \times 10^5$ K and cosmic abundances at regular intervals of 10^5 K. Dashed line: NLTE model spectrum at $\log g = 9, T_{\rm eff} = 6 \times 10^5$ K and 0.25 times cosmic abundances

2.3. Treatment of collisional rates

The collisional rates are given by ($i < j$):

$$C_{ij} = n_e \Omega_{ij}(T) \tag{3}$$

For hydrogen and helium, $\Omega_{ij}(T)$ is taken from Mihalas et al. (1975). For other elements Seaton's equation for collisional ionization (1964) and van Regemorter's equation for collisional excitation (1962) with $\bar{g} = 0.25$ are used.

3. Results

3.1. Comparison of LTE and NLTE model atmospheres

In Fig. 1 we show spectra from a blackbody, an LTE model atmosphere and a NLTE model atmosphere at $T_{\rm eff} = 6 \times 10^5$ K and $\log g = 8.5$. The abundances are cosmic for both model atmospheres. A comparison between the blackbody and the LTE model has already been made by Heise et al. (1994). Note that, for this particular example, the flux of the LTE model exceeds the flux of the blackbody in the energy range where most SSSs have their peak energies (0.2 - 0.4 keV). NLTE models (when NLTE is important) often decrease the depth of the absorption edge compared to LTE. In Fig. 1 we show that edges can appear in emission: The C VI edge (0.49 keV) is in absorption in the case of LTE whereas this edge is in emission for NLTE. This effect is similar to the He II emission edge reported by Husfeld et al. (1984). The emission edges cause the NLTE soft X-ray spectrum to be no longer cut off at a certain dominant edge as it is in the LTE case, but to contribute considerably to the total flux beyond this edge instead.

Emission edges appear because important opacity sources like hydrogen and helium are completely ionized at the temperatures of interest ($\geq 5 \times 10^5$ K) such that other *almost* completely ionized ions, like C VI, become the dominant opacity source. Since the opacity of such ions is only weak, the optical depth $\tau_\nu = 2/3$ on both sides of an ionization edge occurs at practically the same geometrical depth. This has the following consequences for the Planck function and the scattering source function (the low- and high-energy side of the edge are indicated by - and + respectively):

$$n_{\rm e,-} \approx n_{\rm e,+} \Rightarrow S_-^{\rm scat} \approx S_+^{\rm scat}, \tag{4}$$

$$T_- \approx T_+ \Rightarrow B(T_-) \approx B(T_+). \tag{5}$$

It is essential that the scattering source function, which is by far the dominant part of the total source function, remains constant at the depth of continuum formation. The thermal source function changes considerably over the ionization edge:

$$S_-^{\rm th} = \frac{\sum \eta_-}{\sum \chi_-} \approx B(T), \tag{6}$$

$$S_+^{\rm th} = \frac{\sum \eta_- + \eta_{\rm C\,VI}}{\sum \chi_- + \chi_{\rm C\,VI}} \approx \frac{\eta_{\rm C\,VI}}{\chi_{\rm C\,VI}} = \frac{\eta^*_{\rm C\,VI}}{b\chi^*_{\rm C\,VI}} = \frac{B(T)}{b}, \tag{7}$$

where η and χ are the emission and absorption coefficient respectively, b is the departure coefficient corresponding to the ionization edge according to Menzel & Cillié (1937) and $*$ denotes LTE quantities. Because, for this C VI transition, $b < 1$,

$$S_-^{\rm th} < S_+^{\rm th} \;\Rightarrow\; S_-^{\rm tot} < S_+^{\rm tot}, \tag{8}$$

and the ionization edge appears in emission. This effect depends crucially upon the presence of *almost* completely ionized ions which nevertheless are the dominant opacity sources. For strong opacity sources,

$$n_{\rm e,-} > n_{\rm e,+} \Rightarrow S_-^{\rm scat} > S_+^{\rm scat} \tag{9}$$

because optical depth $\tau_\nu = 2/3$ occurs at different geometrical depths. The change in scattering source function dominates over any change in thermal source function:

$$(S_-^{\rm scat} + S_-^{\rm th}) > (S_+^{\rm scat} + S_+^{\rm th}) \;\Rightarrow\; S_-^{\rm tot} > S_+^{\rm tot} \tag{10}$$

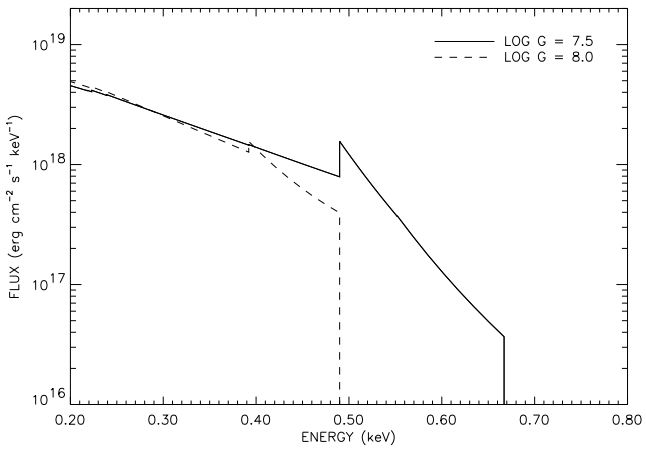

Fig. 3. NLTE model spectra at $T_{\rm eff}$ = 4×10^5 K and $\log g$ = 7.5 and 8. Abundances are cosmic. Note the C VI edge (0.49 keV) turning from emission to absorption when gravity is increased

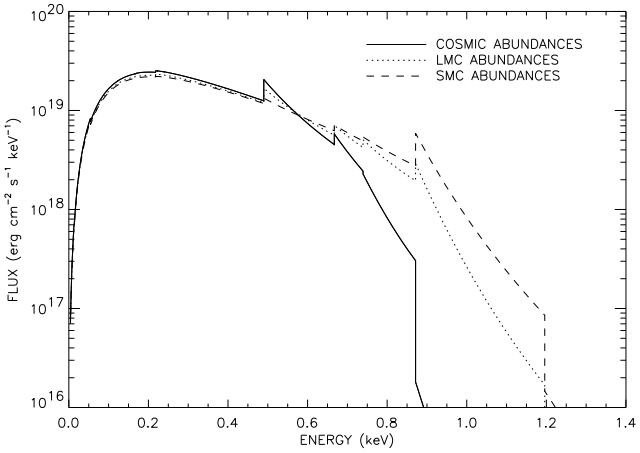

Fig. 4. NLTE model spectra at several abundances. $T_{\rm eff}$ = 6.5×10^5 K and $\log g$ = 8.5. Note the O VIII edge (0.87 keV) turning from absorption to emission when the metallicities are decreased

and the edge appears in absorption. We expect that the emission edges may also disappear when other strong opacities are included, e.g. in the case of line blanketing (cf. Rauch 1996).

3.2. Dependence on temperature and gravity

Increasing the temperature shifts the ionization equilibrium towards higher degree of ionization. Emission edges appear at higher ionization stages as they become *almost* completely ionized. See Fig. 2. Conversely, increasing the gravity increases the atmospheric density, shifting the ionization equilibrium towards lower degree of ionization (according to the Saha-law). This causes emission edges to turn to absorption. This is shown in Fig. 3. Note that the soft X-ray flux beyond the C VI edge (0.49 keV) is much higher for $\log g$ = 7.5 than for $\log g$ = 8. At even higher gravity ($\log g > 9$), higher densities cause collisional ionizations to dominate over photoionizations. The radiation field is more strongly coupled to the local temperature. In that case, the emitted spectrum resembles an LTE spectrum.

3.3. Dependence on abundances: cosmic, LMC and SMC

In order to check on the effect of abundances we demonstrate NLTE models with cosmic, LMC and SMC abundances. In general, the metallicities of the LMC are roughly 0.25 times cosmic and those of the SMC are roughly 0.15 times cosmic (for more details see Dennefeld 1989). In Fig. 4 we show spectra with $T_{\rm eff}$ = 6.5×10^5 K and $\log g$ = 8.5.

Note the influence on the spectrum of the O VII (0.74 keV) edge and the O VIII (0.87 keV) edge turning from absorption to emission when the metallicities are reduced. Evidently the soft X-ray flux beyond the O VIII (0.87 keV) edge is much lower for cosmic abundances compared to LMC and SMC abundances.

The depths of the absorption edges are decreased (and even turn to emission) since the lower metallicity causes less absorption of radiation beyond those edges.

In Fig. 2 we demonstrate a NLTE model spectrum at $T_{\rm eff}$ = 6×10^5 K, $\log g$ = 9 and 0.25 times cosmic abundances (dashed line). It shows a strong resemblance with the $T_{\rm eff}$ = 6×10^5 K, $\log g$ = 8.5 model spectrum at cosmic abundances.

4. Model atmosphere fits

We fit the ROSAT PSPC data of the SSSs CAL87 and RX J0925.7-4758 to NLTE model atmospheres. The luminosities are determined assuming spherically symmetric emission. CAL87 and RX J0925.7-4758 are found to be extremely hot SSSs. The results are compared with earlier blackbody fits. Both CAL87 and RX J0925.7-4758 are scheduled for observation with the Italian/Dutch X-ray satellite SAX. The spectral resolution of SAX (LECS) at 1keV $\approx$ 20% FWHM.

CAL87 was discovered in the Einstein LMC survey (Long et al. 1981). It was observed in two pointed observations by the ROSAT PSPC in February 1991 at a count rate of 0.12 cts s^{-1} with a total observation time of 37.6 ksec (Schmidtke et al. 1993). The optical counterpart of CAL87 has been identified with a $18^{\rm m}$ late F or early G type star. From optical observations van den Heuvel et al. (1992) estimated the mass $M \approx 1.4 - 1.5\ {\rm M}_\odot$. The optical spectrum shows a very blue continuum with the He II 4686 line and H_α in emission characteristic for radiation from an accretion disc (Pakull et al. 1988). The systemic velocity is $\sim$ 306 km s^{-1} which is similar to the mean value of the LMC velocity. This is the best evidence that CAL87 is a member of the LMC.

CAL87 is a binary with a period of $10.6^{\rm h}$. The optical light curve shows a deep asymmetric primary minimum and a shallow, variable secondary minimum. The asymmetry is probably due to the geometry of the accretion disc (Schandl et al. 1996). The binary system is observed at high inclination, $i = 70^\circ - 90^\circ$, and therefore the central object is shrouded by

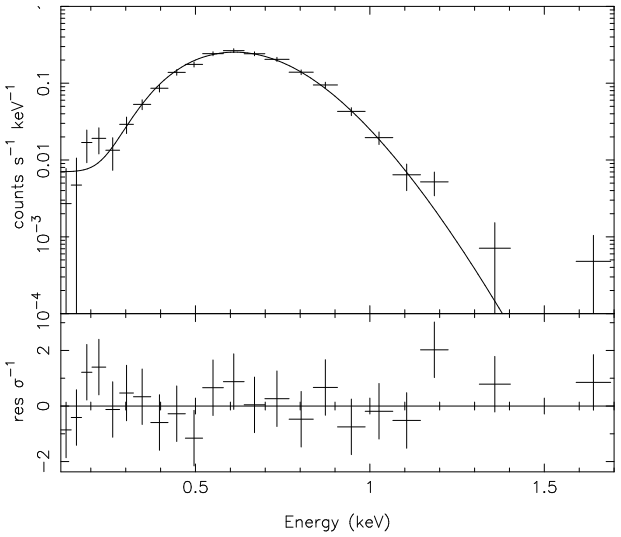

Fig. 5. NLTE model atmosphere fitted to the LMC SSS CAL87. For fit parameters see Table 2

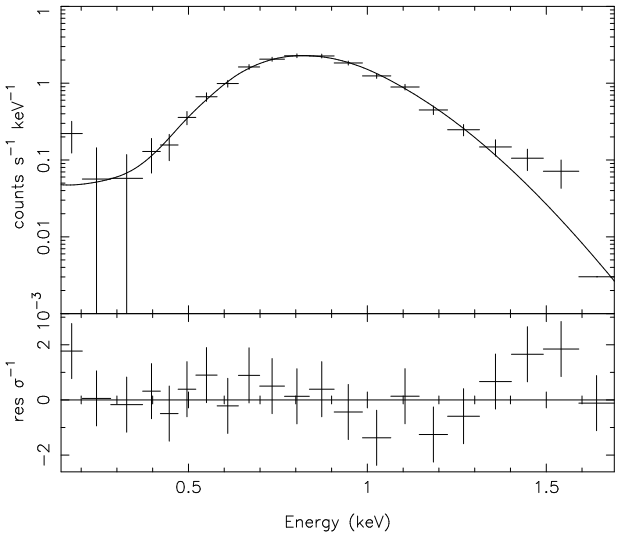

Fig. 6. NLTE model atmosphere fitted to the galactic SSS RX J0925.7-4758. For fit parameters see Table 2

the rim of the accretion disc. The observed X-ray luminosity of $L_X = 10^{36}$ erg s^{-1} is probably due to irradiation of this accretion disc. The intrinsic X-ray luminosity of the central object is assumed to be $\sim 4 \times 10^{37} - 10^{38}$ erg s^{-1}. A shallow eclipse in X-rays is present at primary optical minimum (Schmidtke et al. 1993).

CAL87 has a blackbody temperature of ~ 35 eV assuming a column density of 10^{22} cm^{-2}. Assuming a distance to the Large Magellanic Cloud of 52 kpc, Heise et al. (1996) fitted CAL87 with LTE model atmospheres and found a temperature of 63-84 eV, a luminosity of $1.1 \times 10^{37} - 10^{38}$erg s^{-1} at a column density of $(2.4 - 5) \times 10^{21}$ cm^{-2}. We fitted CAL87 with NLTE model atmospheres and found a temperature of 52 eV, a luminosity of 1.9×10^{38}erg s^{-1} at a column density of 5.6×10^{21} cm^{-2} ($\chi^2 = 0.77$), see Table 2 and Fig. 5.

RX J0925.7-4758 is a galactic supersoft source, discovered in the ROSAT galactic plane survey (Motch et al. 1991). It was reobserved in two pointed observations on 20 November 1993 by ROSAT PSPC and on 23 November 1993 by ROSAT HRI. The total exposure time of all observations was only 7.8 ksec. The PSPC count rate of 1.0 cts s^{-1} shows evidence for variability on timescales of ~ 3.5 hours (Motch et al. 1994). RX J0925.7-4758 has been spectroscopically identified with a $17^{\rm m}$ star with spectral features which resemble those of conventional LMXBs. RX J0925.7-4758 has a bolometric luminosity close to the 1 $M_\odot$ white dwarf Eddington limit. The companion is possibly a $1.5 - 2.5$ $M_\odot$ main sequence star (cf. van den Heuvel et al. 1992).

The RX J0925.7-4758 ROSAT data have been fitted with blackbody spectra at temperatures between $40 - 55$ eV, a high column density of 1.3×10^{22} cm^{-2}, and a (blackbody) luminosity of 2×10^{38} erg s^{-1}. This luminosity and column density constrain the distance of RX J0925.7-4758 between 425 and 2000 pc assuming that intrinsic absorption is not a general feature for SSSs (Motch et al. 1994).

We fitted RX J0925.7-4758 with NLTE model atmospheres and found a temperature of 72 eV, a luminosity of 5.0×10^{35}erg s^{-1} at a column density of 1.0×10^{22} cm^{-2} ($\chi^2 = 0.78$). There is a significant excess in the data above 1.3 keV which does not show up in the folded model spectrum. See Table 2 and Fig. 6.

RX J0925.7-4758 was observed by ASCA in November 1994. Ebisawa et al. (1996a) imposed four edges to the blackbody spectrum fitted to the ASCA data. The fit could thus be improved. Ebisawa et al. derived a temperature of 96 eV and a radius of the compact object of 140 km, see Table 2. So far all fits to RX J0925.7-4758 have resulted in a small radius of a few hundred kilometers.

5. Discussion

For $\log g < 9$ it appears that NLTE model atmospheres differ considerably from LTE model atmospheres. LTE model spectra show strong absorption edges at dominant ions, whereas those edges can even be in emission in NLTE depending on the effective temperature, gravity and abundance. The presence of emission edges is strongly influenced by the effective temperature. At relatively low temperatures ($\sim 3 \times 10^5$ K) the NLTE model spectra resemble the LTE model spectra, since the LTE spectra are no longer cut off by strong absorption edges that occur at higher temperatures. Folding those low temperature models with the low energy resolution of ROSAT PSPC, the edges, either in absorption or emission, are smeared out and both models result in similar quality fits.

At increasing gravity the emission edges gradually disappear and turn into absorption edges. At the increased density the collisional ionizations start to dominate over photoionizations

Table 2. Fit parameters for the SSSs CAL87 and RX J0925.7-4758

	kT (eV)	log $N_{\rm H}$ (cm^{-2})	log L (erg sec^{-1})	log R (cm)	log g (cm s^{-2})
CAL87 :					
NLTE	52	21.7	38.3	9.2	9
LTE[1]	63-84	21.7-21.4	38.0-37.0	8.9-8.1	8.25-9.9
Blackbody	35	22.0	38.0	9.4	–
RX J0925.7-4758 :					
NLTE	72	22.0	35.7	7.6	9
LTE	93	22.0	35.5	7.3	9.25
Blackbody	40-55	22.1	38.3	7.4-7.1	–
bb + edges[2]	96	22.0	35.3	7.1	–

[1]Heise et al. (1996), [2]Ebisawa et al. (1996a)

and LTE is restored. Still the spectra differ significantly from LTE model atmospheres at the same temperature and gravity, so one should be careful assuming that LTE is a good approximation at high gravity. It is worthwhile to investigate whether this assumption becomes valid at even higher gravities, e.g. in the inner parts of accretion discs around neutron stars where the gravity component perpendicular to the disc has $\log g \gg 9$.

The abundances have an important impact upon the shape of the spectrum. At low metallicities emission edges show up, which is not the case at high metallicities. We hope to be able to put constraints on the abundances of SSSs in the near future. A first glance at $\log g = 10$ model spectrum fits suggests low metal abundances for RX J0925.7-4758 (Ebisawa et al. 1996b).

The first conclusion is that the modest spectral resolution of proportional counters does not allow to uniquely determine the spectrum of SSSs. Several combinations of effective temperature, gravity and abundances, when folded with the detector response, fit the observations. It is therefore necessary to have additional information about the source, e.g. better spectral resolution, observations in other wavelengths or on theoretical grounds, in order to constrain the free parameters and to be able to determine effective temperatures and luminosities unambiguously. The second conclusion that can be drawn is that the NLTE model spectrum is not cut off at a certain dominant edge, as is the case for LTE models, since the depths of the edges are decreased or even in emission. This effect is important for soft X-ray sources which emit a considerable amount of their flux above this cutoff energy. These sources can be fitted with models at lower temperatures because NLTE models are more efficient X-ray emitters than LTE models above the cutoff energy. The luminosities are comparable to the LTE luminosities because NLTE models fit a somewhat higher radius.

The luminosity of CAL87 cannot be calculated assuming spherical symmetry since the accretion disc shields part or all of the emitted flux from the central object. The luminosities in Table 2 may therefore be too low, though they are close to the Eddington limit. There is no indication that the difference between the observation and the model spectrum of CAL87 at ~ 1.2 keV is significant.

The difference between the observed spectrum of RX J0925.7-4758 and the fitted model above ~ 1.3 keV is due to the strong Ne IX edge in the unfolded model at 1.2 keV that cuts off the spectrum (Ebisawa et al. 1996a). RX J0925.7-4758 must be fitted to models with even higher effective temperature and gravity. The obtained radius of 372 km for RX J0925.7-4758 may either indicate that this source is more distant than the assumed 1000 pc, though one would need a distance of 10 kpc to obtain a radius comparable to that of a white dwarf, or only a small fraction of the surface of RX J0925.7-4758 ($\sim 10^{-4}$) is emitting soft X-rays. In the latter case we are either dealing with 'hot spots' or 'hot belts' on the surface of a white dwarf, or RX J0925.7-4758 is partly obscured by an accretion disc. RX J0925.7-4758 may even be an example of a neutron star with an extended atmosphere (Kylafis & Xilouris 1993, Kylafis 1996). A way to distinguish between those two possibilities would be to fit RX J0925.7-4758 with even higher gravity model atmospheres since neutron stars have $\log g \geq 11$ at 372 km distance and massive (O, Ne, Mg) white dwarfs have an upper limit of $\log g \leq 10$.

Acknowledgements. This work has been supported by funds of the Netherlands Organization for Scientific Research (NWO). The authors wish to thank Thierry Lanz for his contribution to the discussion and for carefully reading this manuscript.

References

Allen, C.W. 1973, *Astrophysical quantities*, The Athlone Press, University of London

Barfield, W.D., Koontz, G.D. & Huebner, W.F. 1972, J.Quant. Spec. Rad. Transf. 12, 1409

Dennefeld, M. 1989, Abundances from gaseous nebulae in the Magellanic Clouds, in: *Recent developments of Magellanic Cloud research*, de Boer, K.S., Spite, F. & Stasińska, G. eds., Paris

Dreizler, S. & Werner, K. 1993, A&A 278, 199

Ebisawa, K., Asai, K., Mukai, K., Smale, A., Dotani, T., Hartmann, H.W. & Heise, J. 1996, X-ray energy spectrum of RX J0925.7-4758 with ASCA, in: *Supersoft X-ray Sources*, ed. J. Greiner, Lecture Notes in Physics 472, Springer, 91

Ebisawa, K. et al. 1996, in preparation

Heise, J., van Teeseling, A. & Kahabka, P. 1994, A&A 288, L45
Heise, J., van Teeseling, A. & Kahabka, P. 1996, A&A in preparation
Henry, R.J.W. 1970, ApJ 161, 1153
Van den Heuvel, E.P.J., Bhattacharya, D., Nomoto K. & Rappaport S.A. 1992, A&A 262, 97
Hubený, I. 1988, Comput. Phys. Commun. 52, 103
Hubený, I. & Lanz, T. 1995, ApJ 439, 875
Husfeld, D., Kudritzki, R.P., Simon, K.P. & Clegg, R.E.S 1984, A&A 134, 139
Jordan, S., Mürset, U. & Werner, K. 1994, A&A 283, 475
Jordan, S., Schmutz, W., Wolff, B., Werner, K. & Mürset, U. 1996, A&A 312, 897
Kylafis, N.D. 1996, Neutron stars can do it too if they want to, in: *Supersoft X-ray Sources*, ed. J. Greiner, Lecture Notes in Physics 472, Springer, 41
Kylafis, N.D. & Xilouris, E.M. 1993, A&A 278, L43
Lanz, T. & Hubený, I. 1995, ApJ 439, 905
Long, K.S., Helfand, D.J. & Grabelsky, D.A. 1981, ApJ 248, 925
Menzel, D.H. & Cillié, G.G. 1937, ApJ 85, 88
Mihalas, D., Heasley, J.N. & Auer, L.H. 1975, A Non-LTE model stellar atmosphere computer program (NCAR-TN/STR-104)
Motch, C., et al., 1991, A&A 246, L24
Motch, C., Hasinger, G. & Pietsch, W. 1994, A&A 284, 827
Pakull, M.W., Beuermann, K., van der Klis, M. & van Paradijs, J. 1988, A&A 203, L27
Rauch, T. 1996, Implications of light metals (Li-Ca) on NLTE model atmospheres for hot stars, in: *Supersoft X-ray Sources*, ed. J. Greiner, Lecture Notes in Physics 472, Springer, 139
Van Regemorter, H. 1962, ApJ 136, 906
Reilman, R.F. & Manson, S.T. 1979, ApJS 40, 815
Schandl, S., Meyer-Hofmeister, E. & Meyer, F. 1996, A&A submitted
Schmidtke, P.C., McGrath, T.K., Cowley, A.P. & Frattare, L.M. 1993, PASP 105, 863
Seaton, M.J. 1964, Planet. & Sp. Sci. 12, 55
Verner, D.A. & Yakovlev, D.G. 1995, A&AS 109, 125

This article was processed by the author using Springer-Verlag LaTeX A&A style file *L-AA* version 3.